IDENTIFICATION OF WIRELESS USERS VIA POWER AMPLIFIER IMPERFECTIONS

Sepideh Dolatshahi[*]

Georgia Institute of Technology
School of Electrical and Computer Engineering
sepideh@gatech.edu

Adam Polak, Dennis L. Goeckel[†]

University of Massachusetts Amherst
Electrical and Computer Engineering Department
apolak@engin.umass.edu, goeckel@ecs.umass.edu

ABSTRACT

Variations in the RF chain of radio transmitters can be used as a signature to uniquely associate wireless devices with a given transmission. Previous approaches, which have varied from transient analysis to machine learning, do not provide verifiable accuracy. Here, we detail a first step toward a model-based approach. In particular we exploit differences in nonlinearities of input/output (I/O) characteristics of power amplifiers modeled with Volterra series and develop algorithms for deciding the origin of a given message of interest based on these differences. We consider a generalized likelihood ratio test (GLRT) and a classical likelihood ratio test. For both tests, decision rules are derived and their performance is analyzed. Finally, to establish the viability of the proposed approach, the practical variations among power amplifiers are investigated through simulations and measurements. Results show that the methods can be very effective, when exploiting imperfections of commercially used RF power amplifiers (PAs).

Index Terms— Radiometric identification, Volterra series, GLRT, breaking anonymity, process variations

1. INTRODUCTION

The Internet provides new crime opportunities and crime types. The sexual exploitation of children, production and dissemination of contraband music and video, intellectual property theft, identity theft, financial fraud and espionage are some instances of crimes either created or made easier by the advent of computers and use of the Internet. In particular, use of open wireless access points (APs) hosted by private homes, businesses, and municipalities provides offenders with significant anonymity. Fortunately, the use of computers by such offenders typically results in digital evidence. Artifacts used conventionally for identification of users in the wired Internet are Internet Protocol (IP) address and Media Access Control address (MAC address). However MAC addresses can be easily manipulated via software and IP addresses in wireless access networks are assigned to users only temporarily. Thus both of these artifacts are useless when applied for users' identification in wireless networks.

At the physical layer, despite decades of significant efforts by the microwave circuits community, there still exist longstanding imperfections in the RF portion of the wireless transmitter. Furthermore, since these cannot be altered by the user without significant effort, they can be exploited to group together signals from one radio. The different elements in the simplified model of a transmit chain for a wireless transmitter, including the digital-to-analog converter, the mixer, and the power amplifier, show nonidealities, which can be used as radiometric signatures of individual users. Because power amplifiers are the last elements in the RF chain, which are most difficult for a user to modify via software (or even baseband) control, our investigation starts there.

There has been a number of Radio Frequency Fingerprinting efforts over the years. Much of the work done by the microwave circuit community was focused on the detection and analysis of transients (e.g. [1, 2]). The nature of transients is such that they are difficult to detect and to describe in a succinct way. There has also been a few works in the networking community, on location identification (e.g. [3, 4]), which would allow one to group transmissions from a stationary user. In their recent work [5] Brik et al used machine learning techniques on collected modulation data to train data-agnostic classifiers that are then able to distinguish wireless cards - even when produced by the same vendor. We follow the latter approach, but avoid machine learning techniques, because they do not provide the insight we desire, and more importantly, because they do not provide provable bounds on accuracy as is needed for admissibility in court.

2. PROBLEM STATEMENT

For simplicity the case where two users are connecting to a wireless access point is considered, but the generalization to the more practical case of n users is straightforward using n-hypothesis detection techniques. Figure 1 presents the considered two-users scenario. Since the access point decodes the

[*]The first author performed this work while at University of Massachusetts Amherst.

[†]This paper is based in part upon work supported by the National Science Foundation under grant CNS-0905349.

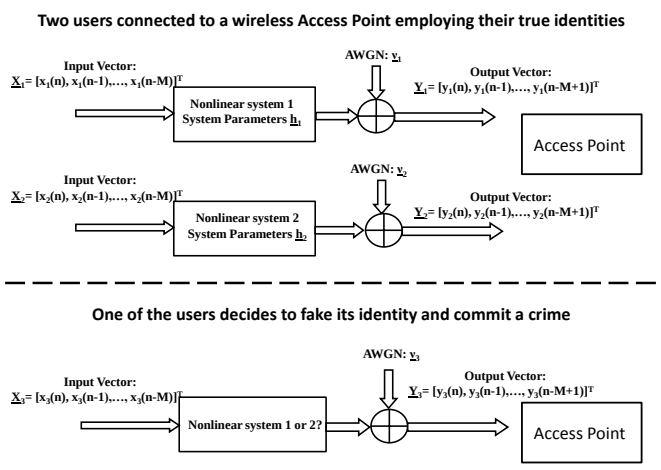

Fig. 1. The two-system identification scenario

packets from each of the users, we assume that we have access to input samples and the corresponding noise-corrupted output samples of the PAs. Denote the input vectors of user one and user two as $\underline{\boldsymbol{X}}_1$ and $\underline{\boldsymbol{X}}_2$ respectively and their respective output vectors as $\underline{\boldsymbol{Y}}_1$ and $\underline{\boldsymbol{Y}}_2$. These correspond to the case where the users are employing their true identities, which they assume at some time when they are not committing a crime. Now, at some point in time, one of the users decides to fake its identity and to commit a crime. The binary hypothesis problem is to identify this user given access to $\underline{\boldsymbol{X}}_i$ and $\underline{\boldsymbol{Y}}_i$, $i = 1, 2, 3$.

3. MODELING CHARACTERISTICS OF POWER AMPLIFIERS

The nonlinear I/O characteristics of PAs are modeled with their Volterra series representation, as well-established in the microwave literature (see Chapter 4 of [6]). For the sake of exposition, a Volterra series representation with memory of one and order of two (a linear quadratic system) is considered, but the extension to higher memory and orders is straightforward. Hence:

$$y_i(n) = \Sigma_{k_1=0}^{1} h_{i,1}(k_1)x_i(n-k_1)+$$
$$\Sigma_{k_1=0}^{1}\Sigma_{k_2=0}^{1} h_{i,2}(k_1,k_2)x_i(n-k_1)x_i(n-k_2)+\nu_i(n)$$

$$y_i(n) = h_{i,1}(0)x_i(n) + h_{i,1}(1)x_i(n-1)$$
$$+h_{i,2}(0,0)x_i^2(n)+h_{i,2}(1,1)x_i^2(n-1)+h_{i,2}(0,1)x_i(n)x_i(n-1)+\nu_i(n) \quad (1)$$

The system parameters vector $\underline{\boldsymbol{h}}_i$ characterizing user i is an $N \times 1$ vector containing Volterra coefficients of the user's I/O characteristic. For the considered Volterra representation $N = 5$ and:

$$\underline{\boldsymbol{h}}_i = \begin{bmatrix} h_{i,1}(0) & h_{i,1}(1) & h_{i,2}(0,0) & h_{i,2}(1,1) & h_{i,2}(0,1) \end{bmatrix}^T$$

For the additive white Gaussian noise (AWGN) channel, based on (1) we obtain the following I/O matrix equation:

$$\underline{\boldsymbol{Y}}_i = P_i\underline{\boldsymbol{h}}_i + \underline{\boldsymbol{\nu}}_i \quad ; \quad i = 1, 2, 3 \quad (2)$$

where

$$P_i = \begin{bmatrix} x_i(n) & x_i(n-1) & \cdots & x_i(n-M+1) \\ x_i(n-1) & x_i(n-2) & \cdots & x_i(n-M) \\ x_i^2(n) & x_i^2(n-1) & \ddots & \vdots \\ x_i^2(n-1) & x_i^2(n-2) & \ddots & \vdots \\ x_i(n)x_i(n-1) & x_i(n-1)x_i(n-2) & \cdots & x_i(n-M+1)x_i(n-M) \end{bmatrix}^T \quad (3)$$

$\underline{\boldsymbol{h}}_i$ is the parameter vector and $\underline{\boldsymbol{\nu}}_i$ is the noise vector.

4. ALGORITHMS

Two algorithms are introduced to solve hypothesis testing problem presented in Section 2. The first algorithm relies on the generalized likelihood ratio test (GLRT). The second one first estimates the Volterra coefficients based on the input and output vectors using least squares (LS) estimation and then solves the resulting detection problem using the classical likelihood ratio test.

4.1. Algorithm 1: Generalized Likelihood Ratio Test

The decision rule of the generalized likelihood ratio test (with an assumption of equally probable hypotheses) can be expressed as:

$$max_{\underline{\boldsymbol{h}}_1}\{p(\underline{\boldsymbol{Y}}_1, \underline{\boldsymbol{Y}}_3 \,|\, \underline{\boldsymbol{h}}_1, \underline{\boldsymbol{X}}_1, \underline{\boldsymbol{X}}_3)\} \underset{\underline{\boldsymbol{h}}_2}{\overset{\underline{\boldsymbol{h}}_1}{\gtrless}} max_{\underline{\boldsymbol{h}}_2}\{p(\underline{\boldsymbol{Y}}_2, \underline{\boldsymbol{Y}}_3 \,|\, \underline{\boldsymbol{h}}_2, \underline{\boldsymbol{X}}_2, \underline{\boldsymbol{X}}_3)\} \quad (4)$$

After substituting the corresponding probability density functions and simplifying the formulas this decision rule can be rewritten as:

$$\underline{\boldsymbol{Y}}_{13}^H(I_{2M\times 2M} - P_{13}(P_{13}^HP_{13})^{-1}P_{13}^H)\underline{\boldsymbol{Y}}_{13} \underset{\underline{\boldsymbol{h}}_1}{\overset{\underline{\boldsymbol{h}}_2}{\gtrless}} \underline{\boldsymbol{Y}}_{23}^H(I_{2M\times 2M} - P_{23}(P_{23}^HP_{23})^{-1}P_{23}^H)\underline{\boldsymbol{Y}}_{23} \quad (5)$$

where P_{i3} and $\underline{\boldsymbol{Y}}_{i3}$ are obtained by stacking the matrices P_i, P_3 and vectors $\underline{\boldsymbol{Y}}_i$, $\underline{\boldsymbol{Y}}_3$ respectively.

To determine the performance of this method and its ability to differentiate between two different transmitters, the expression for probability of error (P_e) should be found in terms of some form of distance between the two system parameters vectors $\underline{\boldsymbol{h}}_1$ and $\underline{\boldsymbol{h}}_2$.

$$P_e = Pr\{\underline{h}_1\} \cdot Pr\{\text{GLRT results: } \underline{h}_2|\underline{h}_1\}$$

$$+Pr\{\underline{h}_2\} \cdot Pr\{\text{GLRT results: } \underline{h}_1 | \underline{h}_2\} \quad (6)$$

Interestingly, after simplifications, this formula can be written in terms of the distance vector $\underline{\boldsymbol{d}} = \underline{\boldsymbol{h}}_2 - \underline{\boldsymbol{h}}_1$:

$$P_e = Pr\{(\underline{\boldsymbol{\nu}} + \underline{\boldsymbol{B}})^H \mathbf{P} \ \ (\underline{\boldsymbol{\nu}} + \underline{\boldsymbol{B}}) < 0\} \quad (7)$$

where:

$$\mathbf{P}_{(3M\times 3M)} = \begin{bmatrix} -(I - P_1 X^* P_1^H) & 0 & P_1 X^* P_3^H \\ 0 & (I - P_2 X P_2) & -P_2 X P_3^H \\ P_3 X^* P_1^H & -P_3 X P_2^H & -P_3 (X - X^*) P_3^H \end{bmatrix}$$

$$\underline{\boldsymbol{B}}_{(3M\times 1)} = \begin{bmatrix} \underline{\mathbf{0}} \\ P_2.\underline{\boldsymbol{d}} \\ \underline{\mathbf{0}} \end{bmatrix} \ ; \ \underline{\boldsymbol{\nu}}_{(3M\times 1)} = \begin{bmatrix} \underline{\boldsymbol{\nu}}_1 \\ \underline{\boldsymbol{\nu}}_2 \\ \underline{\boldsymbol{\nu}}_3 \end{bmatrix}$$

$$X = \left(P_2^H P_2 + P_3^H P_3\right)^{-1} \quad ; \quad X^* = \left(P_1^H P_1 + P_3^H P_3\right)^{-1}$$

Calculation of expected value of the left side of the inequality from (7), after ignoring the matrix $\mathbf{P}$, which is just a rotation matrix, results in:

$$E\left\{(\underline{\boldsymbol{\nu}} + \underline{\boldsymbol{B}})^H (\underline{\boldsymbol{\nu}} + \underline{\boldsymbol{B}})\right\} = M(\sigma_v^2 + WS) \quad (8)$$

where WS is a weighted sum of the components of the vector $\underline{\boldsymbol{d}}$, which for elements of input vectors modeled as realizations of $\sim \mathcal{N}(0, \sigma_x^2)$ random variables, has the form:

$$WS = \underline{\boldsymbol{d}}(1)^2 \cdot \sigma_x^2 + \underline{\boldsymbol{d}}(2)^2 \cdot \sigma_x^2 + \underline{\boldsymbol{d}}(3)^2 \cdot 2\sigma_x^4 + \underline{\boldsymbol{d}}(4)^2 \cdot 2\sigma_x^4 + \\ + (\underline{\boldsymbol{d}}(3) + \underline{\boldsymbol{d}}(4))^2 \cdot \sigma_x^4 + \underline{\boldsymbol{d}}(5)^2 \cdot \sigma_x^4 \quad (9)$$

Eq. (9) shows how the importance of different coefficients changes with the standard deviation σ_x of the elements of the input vectors. For large values of σ_x, the elements of the Volterra representation that model nonlinearities are more important. This is intuitively correct since the increase of the input power should allow for better exploitation of the differences in nonlinearities of the two considered units. The form of the weighted sum in general depends on the chosen Volterra series representation. Eq. (9) is valid for the Volterra representation from (1).

4.2. Algorithm 2: Classical Likelihood Ratio Test

Per above, the algorithm's input are three input/output vector pairs: $\underline{\boldsymbol{X}}_i, \underline{\boldsymbol{Y}}_i, i = 1, 2, 3$. The first two pairs come from nonlinear systems 1 and 2, and it needs to be determined which of the systems the third input/output pair belongs to.

It is more practical to store the estimated system coefficients (coefficients of Volterra series representation of I/O characteristic) $\hat{\underline{\boldsymbol{h}}}_i, i = 1, 2, 3$, rather than having to store all the input and output data. The relation between the data signals $\underline{\boldsymbol{X}}_i, \underline{\boldsymbol{Y}}_i$ and the estimated coefficients is:

$$\underline{\boldsymbol{Y}}_i = P_i \hat{\underline{\boldsymbol{h}}}_i + \underline{\boldsymbol{e}}_i \quad ; \ i = 1, 2, 3.$$

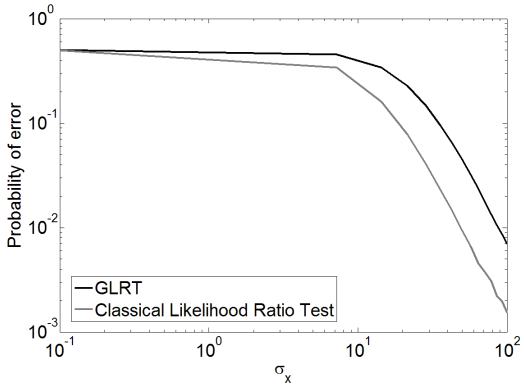

Fig. 2. Probability of error vs. standard deviation of the elements of the input vectors averaged over 500 different input vectors of size $M = 100$ and over 500 randomly generated Volterra vector pairs, with standard deviation of elements $\sigma_h = 10^{-3}$; $SNR = 30dB$.

where $\underline{\boldsymbol{e}}_i$ is the observation error and the $M \times N$ matrices P_i are defined as in (3).

A standard estimation approach is to minimize the squared estimation error. The resulting problem is the classical Least Squares (LS) problem and the solution is:

$$\hat{\underline{\boldsymbol{h}}}_{i,opt} = P_i^{\dagger} \underline{\boldsymbol{Y}}_i = (P_i^H P_i)^{-1} P_i^H \underline{\boldsymbol{Y}}_i, \quad i = 1, 2, 3$$

Now with estimated $\hat{\underline{\boldsymbol{h}}}_{i,opt}$ the decision problem (again with the assumption of equally probable hypotheses) can be solved using the likelihood ratio:

$$\Lambda(\underline{\boldsymbol{h}}_3) \triangleq \frac{p_{\hat{\underline{\boldsymbol{h}}}_{3,opt}|\hat{\underline{\boldsymbol{h}}}_{1,opt}}(\hat{\underline{\boldsymbol{h}}}_{3,opt}|\hat{\underline{\boldsymbol{h}}}_{1,opt})}{p_{\hat{\underline{\boldsymbol{h}}}_{3,opt}|\hat{\underline{\boldsymbol{h}}}_{2,opt}}(\hat{\underline{\boldsymbol{h}}}_{3,opt}|\hat{\underline{\boldsymbol{h}}}_{2,opt})} \underset{\underline{\boldsymbol{h}}_2}{\overset{\underline{\boldsymbol{h}}_1}{\gtrless}} 1$$

With some algebraic manipulations, the receiver's decision rule simplifies to:

$$(\hat{\underline{\boldsymbol{h}}}_{3,opt} - \hat{\underline{\boldsymbol{h}}}_{1,opt})^H (P_3^H P_3)(\hat{\underline{\boldsymbol{h}}}_{3,opt} - \hat{\underline{\boldsymbol{h}}}_{1,opt}) \underset{\underline{\boldsymbol{h}}_1}{\overset{\underline{\boldsymbol{h}}_2}{\gtrless}} \\ (\hat{\underline{\boldsymbol{h}}}_{3,opt} - \hat{\underline{\boldsymbol{h}}}_{2,opt})^H (P_3^H P_3)(\hat{\underline{\boldsymbol{h}}}_{3,opt} - \hat{\underline{\boldsymbol{h}}}_{2,opt}) \quad (10)$$

with the probability of error:

$$P_e = Pr\left\{\hat{\underline{\boldsymbol{d}}}^H P_3^H P_3 \hat{\underline{\boldsymbol{d}}} + \hat{\underline{\boldsymbol{d}}}^H (P_3^H \underline{\boldsymbol{\nu}}_3) + (P_3^H \underline{\boldsymbol{\nu}}_3)^H \hat{\underline{\boldsymbol{d}}} < 0\right\} \quad (11)$$

Similarly to the GLRT, the performance of the classical likelihood ratio test depends on the same weighted sum (9) of elements of vector $\hat{\underline{\boldsymbol{d}}} = \hat{\underline{\boldsymbol{h}}}_{2,opt} - \hat{\underline{\boldsymbol{h}}}_{1,opt}$

Figure 2 shows the simulated probability of error for both methods, for $SNR = 30dB$, versus the standard deviation σ_x of the elements of the input vectors. For generation of the Volterra vector pairs, random vectors with normally distributed elements ($\mu_h = 0, \sigma_h^2 = 10^{-6}$) were added to a vector: [1 0.01 0.01 0.01 0.01].

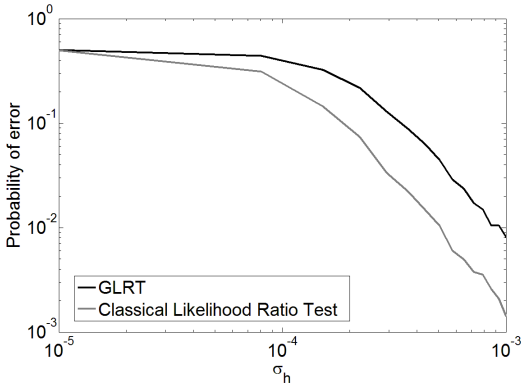

Fig. 3. Probability of error vs. standard deviation of the Volterra coefficients averaged over 2000 randomly generated Volterra vector pairs and 100 different input vectors of size $M = 100$, with standard deviation of the elements $\sigma_x = 100$; $SNR = 30dB$.

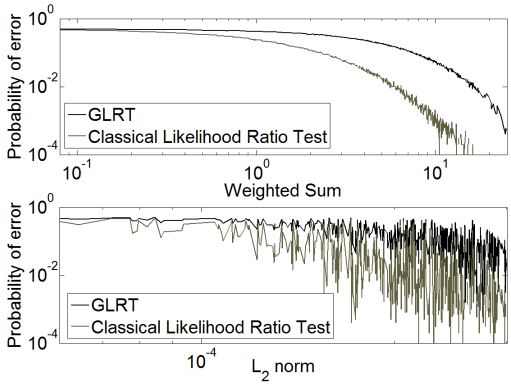

Fig. 4. Probability of error vs. weighted sum- metric that combines differences in the Volterra coefficients and the power of the input signal (upper plot) and vs. L_2 norm of vector $\underline{\boldsymbol{d}}$- metric that takes into account only differences in the Volterra coefficients (lower plot).

Figure 3 also shows simulated P_e, but this time the standard deviation of the elements of the input vectors and the SNR were kept constant ($\sigma_x = 100$, $SNR = 30dB$) and the standard deviation of elements of the random vectors for Volterra vector pairs generation σ_h was varied in the range $\sigma_h \in (0, 0.001)$.

Figures 2 and 3 demonstrate that performance of the methods increases when the power of input signals goes up and when the differences among amplifiers get bigger. But speaking more strictly, the methods perform better when the value of the weighted sum from (9) increases. For two pairs for which the distance between their Volterra coefficients vectors is the same in the sense of the L_2 norm, the methods can yield different probabilities of errors depending on the power of the input signal. Thus for a complete analysis of the performance of the methods, differences in the Volterra series representations should always be considered together with the input power range. Figure 4 shows P_e as a function of the weighted sum (upper plot) and the L_2 distance (lower plot) for 500 randomly generated amplifier pairs with $\sigma_h = 2.5 \cdot 10^{-4}$ and with a standard deviation of elements $\sigma_x = 100$. It can be seen that the weighted sum is a much more appropriate metric.

5. MODELING PROCESS VARIATIONS

To be able to validate the effectiveness of the presented techniques in practical applications, it should be determined how the Volterra series representations of power amplifiers, even of these of the same model and from the same manufacturer, differ in practice due to process variations. MOS transistors, which the amplifier circuits are made of, exhibit broad variations in major device parameters among production lots. Process corners represent a three-sigma (standard deviation) variation from nominal values of transistor parameters (e.g. channel length, channel doping concentration, oxide thickness). The variations may occur for many reasons, such as minor changes in the humidity or temperature in the cleanroom, or due to the position of the die relative to the center of the wafer. Changes of the parameters influence transistor switching speed.

A single transistor RF amplifier was simulated in Advanced Design System software. Differences of I/O characteristics were analyzed for two amplifiers having all parameters chosen from the opposite three-sigma corners. In this case the simulated probability of error of both algorithms from Section 4 was close to zero.

RF amplifiers used in communication devices are multistage, multiple transistor amplifiers, and it is highly improbable to have transistors with parameter values from the opposite three-sigma corners. Thus, in addition to the aforementioned simulations, measurements were performed on power amplifier chips commercially used in WLAN transmitters. In particular I/O characteristics of two $MAXIM$ MAX2242 power amplifiers were measured at a frequency of 2.45GHz with a 12.5GHz, 50GSa/s real time oscilloscope. Based on these characteristics, the coefficients of a memoryless forth order Volterra series representation were calculated and normalized to the same value of the linear gain. The following parameter vectors were obtained:

$$\underline{\boldsymbol{h}}_1 = [29.307, 84.324, 682.774, 969.004]$$

$$\underline{\boldsymbol{h}}_2 = [29.307, 69.698, 673.623, 1019.239]$$

and used for simulation of the performance of the algorithms from Section 4. In addition to the two algorithms described in Section 4, another algorithm termed the "Naive Algorithm" was considered. In this algorithm, the detection system outputs the system number for which the estimated coefficient vector $\underline{\hat{\boldsymbol{h}}}_{opt,i}, i = 1, 2$ is closest to the estimated coefficients vector of the masquerading user $\underline{\hat{\boldsymbol{h}}}_{opt,3}$ under a L_2-norm cri-

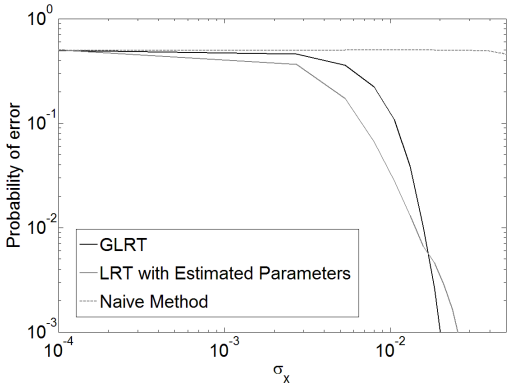

Fig. 5. Probability of error for the measured amplifiers vs. the standard deviation σ_x of the elements of the input vectors averaged over 50000 input vectors of size $M = 100$, SNR equal to $10dB$.

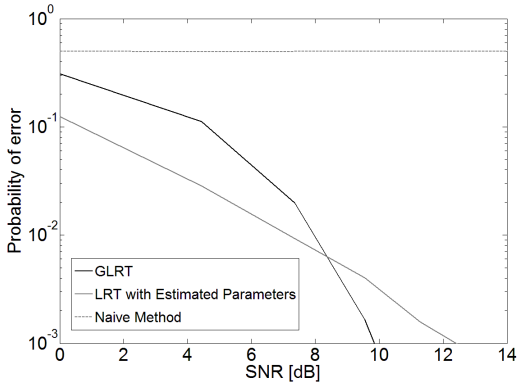

Fig. 6. Probability of error for the measured amplifiers vs. SNR averaged over 50000 input vectors of size $M = 100$, with standard deviation of the elements $\sigma_x = 0.02$.

terion.

$$||\hat{\underline{\boldsymbol{h}}}_{opt,3} - \hat{\underline{\boldsymbol{h}}}_{opt,2}|| \underset{\underline{\boldsymbol{h}}_2}{\overset{\underline{\boldsymbol{h}}_1}{\gtrless}} ||\hat{\underline{\boldsymbol{h}}}_{opt,3} - \hat{\underline{\boldsymbol{h}}}_{opt,1}||$$

Figure 5 shows how the P_e decreased as the standard deviation of the elements of input vectors went up (while the SNR was kept at a constant level of $10dB$). For standard deviation equal to $\sigma_x = 0.02$, the probability of error for the GLRT and the classical likelihood ratio test was low below 1%. For this value of σ_x, the probability that the power of the input signal exceeded -7dBm (upper level of linear range specified by the manufacturer of the considered amplifiers) was only $\approx 1.6 \cdot 10^{-12}$. Techniques proposed in this work exploit only nonlinearities of the amplifier I/O characteristics. Possible differences in the slope of the characteristics are ignored by normalization of the parameter vectors to the same value of the linear gain. This suggests that commercial RF power amplifiers, while being linear enough to meet specifications of communication standards, are non-linear enough to be exploited for purposes of user's identification.

Figure 6 presents P_e as a function of SNR for a standard deviation $\sigma_x = 0.02$ of elements of the input vectors. Figure 6 shows that very low probabilities of errors are achieved for relatively low SNR values.

6. CONCLUSIONS

In this paper, with the motivation of breaking the anonymity of criminals using wireless links, an approach to identify users based on minute imperfections in the different components of the transmitter's hardware was proposed. For the access point case, where the input signal is fully recovered at the receiver, algorithms based on the generalized likelihood ratio test and the classical likelihood ratio test were proposed. By considering the order of variation of the I/O characteristics of RF amplifiers due to production process imperfections, we lend credence to our approach. Continuing work is considering the variation of the characteristics of individual devices over temperature, which greatly complicates identification when based on packet receptions with large temporal separations.

7. ACKNOWLEDGMENT

The authors are indebted to Robert W. Jackson and Arash Mashayekhi from the University of Massachusetts Amherst Laboratory for Millimeter Wave Devices and Applications (LAMMDA) for providing us with the power amplifier simulation data.

8. REFERENCES

[1] J. Hall, M. Barbeau, and E. Kranakis, "Radio frequency fingerprinting for intrusion detection in wireless networks," in *Defendable and Secure Computing*, 2005.

[2] O. Ureten and N. Serinken, "Bayesian detection of radio transmitter turn-on transients," in *NSIP99*, 1999, pp. 830–834.

[3] Y. et al. Chen, "Detecting and localizing wireless spoofing attacks," in *IEEE Conf on Sensor, Mesh and Ad Hoc Comm and Nets (SECON)*. IEEE, June 2007, pp. 193–202.

[4] Patwari N. and Kasera S.K., "Robust location distinction using temporal link signatures," in *ACM MOBICOM*, 2007, pp. 111–122.

[5] V. Brik, S. Banerjee, M. Gruteser, and S. Oh, "Wireless device identification with radiometric signatures," in *Proceedings of the 14th ACM International Conference on Mobile Computing and Networking*, March 2008, pp. 116–127.

[6] P. Wambacq and W. Sansen, *The distortion analysis of analog integrated circuits*, Kluwer, 1998.